Pyridine-based cross-linked chitosan: a biopolymer adsorbent for the green removal of toxic metals from water

Ibraheem Olayiwola Bisiriyu
University of Johannesburg
Reinout Meijboom (rmeijboom@uj.ac.za)
University of Johannesburg https://orcid.org/0000-0003-0901-5690

Research Article

Keywords: selective adsorption, simultaneous adsorption, adsorption energy, DFT

Posted Date: June 8th, 2022

DOI: https://doi.org/10.21203/rs.3.rs-266015/v2

Pyridine-based cross-linked chitosan: a biopolymer adsorbent for the green removal of toxic metals from water

*Ibraheem Olayiwola Bisiriyu and Reinout Meijboom**

Department of Chemical Sciences, University of Johannesburg, PO Box 524, Auckland Park, Johannesburg 2006, South Africa.

Email: rmeijboom@uj.ac.za, bisiriyy@yahoo.com

Abstract

Herein we report the green recovery of toxic metals [namely: Cd^{2+}, Cr^{3+}, Mn^{2+}, Pb^{2+}, and Ni^{2+}] from water utilizing a biopolymer: 2,6-pyridine dicarboxylic acid cross-linked chitosan (PDC-CCS) as the adsorbent. Adsorption studies were performed at varying experimental conditions (such as pH, adsorbent contact time, initial metal ion concentrations, etc.). At the RI-PB/def2-SVP level of theory, the Density Functional Theory (DFT) approach has been used to evaluate the adsorption energy for the metal ions. Selectivity studies were performed at pH 4.20, 5.56, 6.65 and 7.61. While Mn(II), Cd(II) and Ni(II) were strongly adsorbed at higher pH (7.5), Cr(III) and Pb(II) were seen to be strongly adsorbed at lower pH (around 4.0). Selectivity studies revealed that PDC-CCS can be utilized for simultaneous removal of the metals at pH 4.2; selective adsorption of Mn(II) at pH 5.56 as well as simultaneous-selective removal of Ni(II) and Mn(II) near neutral pH. The experimental maximum adsorption limit of PDC-CCS for Ni(II), Cd(II), Pb(II), Mn(II), and Cr(III), were found to be 1258.79, 1118.70 928.52, 829.62 and 580.21 mmol/g respectively. When compared with some relevant previously used adsorbent, PDC-CCS shows an exceptional adsorption capacity. Consequently, a successful biopolymer adsorbent for the treatment of water contaminated by hazardous metals.

Key words: selective adsorption; simultaneous adsorption; adsorption energy; DFT

Indisputably, contamination of water by heavy metals constitutes major environmental problem owing to their debilitating effect and uneasy complete removal. Chitosan [a biopolymer obtained from chitin (figure 1a)] on the other hand is known for its high adsorption property towards metal ions [1]. Likewise, improvement in the sorption property of chitosan [with incomplete deacetylation (figure 1b), fully deacetylated (figure 1c)] has been made possible through several modifications that utilize the free amino function group in chitosan [1]

[2]. Despite the fact that the utilization of chitosan in its modified form for the expulsion of noxious metals from water has pulled in a great deal of interests as of late [3] [4] [5] [6] [7] [8] [9] [10] [11] [12] [13] [14] [15] [16] [17] [18] [19] [20] [21] [22] [23] [24] [25] [26] [27] [28] [29] [30] [31] [32] [33] [34] [35] [36] [37] [38] [39] [40] [41] [42] [43] [44], the utilization of pyridine based cross-linked chitosan has not been accounted for as far as we could possibly know. Recently, we reported a new pyridine based cross-linked chitosan (figure 1d) (2,6-pyridine dicarboxylic acid cross-linked chitosan) as a non-toxic biopolymer adsorbent for the recovery of Cu(II) ions from water [45]. In furtherance to this, the pyridine-based biopolymer has been utilized in this study in order to extract other toxic metals from water, including; cadmium, chromium, manganese, lead, and nickel with the end goal of investigating/researching the selectivity of this adsorbent with regard to the solution pH and the interaction time of the adsorbent at the optimum temperature and the ideal initial metal ions concentration. Additionally, the Density Functional Theory (DFT) approach has been employed to justify the adsorbent's adsorption limit/capacity for each of the metals under scrutiny.

The deacetylation degree of chitosan was determined from previous study [45] by ^{1}H NMR spectroscopy using the formulae:

$$\mathrm{DDA} = \left(1 - \frac{I_{CH_3}}{3 \times \sum I_{H_1}}\right) \times 100\% \quad (1) \quad [46]$$

$$\mathrm{DDA} = \left(\frac{I_{H1-GlnN}}{I_{H1-GlnN} + \frac{1}{3} I_{CH_3}}\right) \times 100\% \quad (2) \quad [47] [48]$$

Where I_{CH_3} depicts the proton integral in –$COCH_3$ group and $\sum I_{H_1} = I_{H1-GlnN}$ this implies the summation of the proton integral attached to the D-glucosamine unit's C1 atom. Chitosan's degree of deacetylation (DDA) was obtained at 96 percent.

In accordance with the updated literature procedure of Sailakshmi et al [49], pyridine-2,6-dicarboxylic acid crosslinked chitosan (PDC-CCS) was prepared, and the cross-linking degree was determined using the bradford assay. The presence of pyridine-2,6-dicarboxylic acid in the PDC-CCS was revealed by ^{13}C NMR and UV-visible spectroscopy through peaks due to aromatic carbons and carbonyl carbons. FT-IR confirmed the interaction of the cross-linker with chitosan at the –NH_2 functional group. Elemental analysis showed an increase in the C/N ratio after cross-linking indicating a successful incorporation of the crosslinker. The result of

the Bradford assay confirmed that the cross-linking is 100% complete. After crosslinking, X-ray diffraction spectroscopy revealed a reduction in the crystallinity of the biomaterial. Thermal analysis suggested a decrease in stability upon cross-linking. N_2 adsorption isotherm and SEM analysis indicated an increased surface area as well as increased porosity of the synthesized cross-linked chitosan [45].

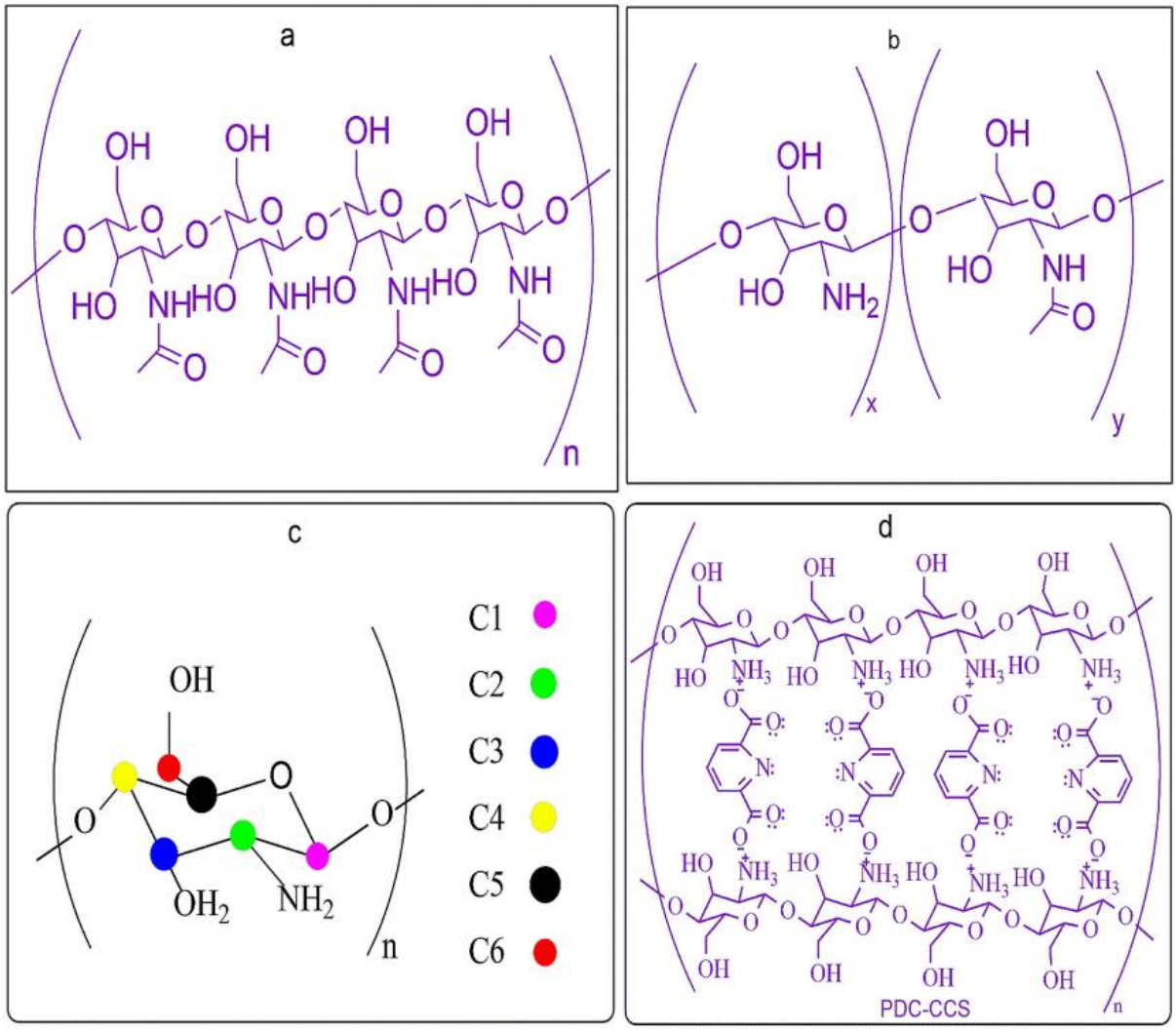

Figure 1: Structure of (a) chitin (b) chitosan (c) fully deacetylated chitosan (d) crosslinked chitosan showing possible binding sites

Following the Thien et al literature approach, we used PDC-CCS from previous research to recover Cu(II) from water [46]. In addition, to obtain an optimal adsorption state, the impact of temperature, the solution pH, adsorbent time of contact along with initial concentration of Cu(II) ions were examined. In fact, the adsorption limit/capacity Q has been evaluated according to equation 3.

$$Q = \frac{V \times (C_o - C)}{W} \quad (3)$$

Where Q, C and C_o are, individually, the adsorption limit/capacity ($mmolg^{-1}$), the final equilibrium concentration of metal ions ($mmoll^{-1}$) and the initial concentration of metal ions. Likewise, the solution volume (l) and sorbent mass (g) are V and W, respectively. Additionally, evaluation of the experimental data has been performed with kinetic models (pseudo-first-order and second-order kinetic models according to equation 4 and 5 respectively) and models of Isothermal Adsorption (Langmuir and Freundlich adsorption isotherms according to equation 6 and 7 respectively)

$$ln(q_e - q_t) = lnq_e - \frac{k_1}{2.303}t \quad (4)$$

$$\frac{t}{q_t} = \frac{1}{k_2 q_e^2} + \frac{t}{q_e} \quad (5)$$

$$\frac{C_e}{Q_e} = \left(\frac{1}{K_L q_m}\right) + \left(\frac{C_e}{q_m}\right) \quad (6)$$

$$lnQ_e = lnk_f + \left(\frac{1}{n}\right) lnC_e \quad (7)$$

Where the quantity of Cu(II) ion adsorbed (mgg^{-1}) at equilibrium and time t is q_e and q_t respectively; The first-order and second-order adsorption rate constants (min^{-1}) are respectively expressed by k_1 and k_2; Ce is the equilibrium Cu(II) ion concentration in solution (mgl^{-1}), whereas the equilibrium adsorption limit/capacity (mgg^{-1}) is denoted as Q_e; for a single-layer coverage (mgg^{-1}), q_m represents the saturated adsorption limit, while k_f, n and K_L are taken as constants. The observed optimum adsorption conditions were: temperature of 30 °C, pH of about 7.5, the initial concentration of Cu(II) ions was found to be 2.5 mM and the contact time was 60 mins. The second-order kinetic model was in good fitness with the experimental adsorption of the Cu(II) ion onto PDC-CCS. Similarly, the Langmuir isothermal adsorption model was adequate for the elucidation of the experimental results. In the same vein, the adsorption process has been shown to be spontaneous and enthalpy driven from the result obtained from the thermodynamic studies of adsorption. In particular, a high value of 2186 mmol/g was obtained for Cu(II) ions as the maximum adsorption limit/capacity of the PDC-CCS. This value was much higher when compared with value obtained from other studies in

the literature. Moreover, PDC-CCS could easily be regenerated and reused for several adsorption cycles [45].

While we expect the adsorption of other metals [Cd^{2+}, Cr^{3+}, Mn^{2+}, $Pb^{2+,}$ and Ni^{2+}] onto the PDC-CCS to follow the same mechanism/model for the recovery of Cu (II), the assessment of the PDC-CCS adsorption potential for each of the metals was first carried out under optimum Cu(II) adsorption conditions before varying the experimental conditions. Solutions of the metal ions [Cd^{2+}, Cr^{3+}, Mn^{2+}, $Pb^{2+,}$ and Ni^{2+}] at the optimum initial concentration were first prepared by dissolving calculated amount of the salts [$CdCl_2 \cdot H_2O$, $Cr(NO_3)_3 \cdot 9H_2O$, $MnCl_2 \cdot 4H_2O$, $(CH_3COO)_2Pb \cdot 3H_2O$ and $NiCl_2$,] separately in distilled water. The metal ions concentrations in the solutions were determined with Spectro Arcos ICP-OES. To change the pH of the solutions to the optimum pH, sodium hydroxide and hydrogen chloride solutions were added where appropriate. In 25 ml of prepared metal ion solutions, 0.005 g of PDC-CCS was added separately with constant shaking at the optimum temperature, and contact time, at some time intervals, a 0.25 ml solution was taken, and the concentrations of the metal ions in the samples were again measured. Based on the difference between the initial and final concentrations of metal ions in aqueous solutions, the adsorption limit for metal ions was calculated at a given time using equation 3.

The adsorbent selectivity for the metal ions in the solution was examined by first preparing a 25 ml solution mixture of Cd^{2+}, Cr^{3+}, Mn^{2+}, Pb^{2+}, Ni^{2+}, and Cu^{2+} at the said ideal concentration of the metal ions by weighing the calculated amount of the respective salts in a graduated vessel and diluting up to the required volume. Aqueous hydrochloric acid/ammonia was used where appropriate to change the solution's pH. Four different solution mixtures of the metal ions were thus prepared with a pH of 4.20, 5.56, 6.65, and 7.61. The initial concentrations of the metal ions were calculated for the four separate solutions using ICP-OES. Thereafter, a 0.005g of the adsorbent (PDC-CCS) was added separately into the four different solutions with continuous shaking at the optimum temperature. Samples from the solutions were taken at intervals of 5, 10, 15, and 20 mins; the concentration of metal ions in the samples was again measured, the capacity of adsorption was calculated, and the selectivity for each metal was examined.

The adsorption energy for each of the metals has been estimated by computing the final single point energy (FSE) of the adsorbent, metal ion in solution, adsorbent-metal complexes, and H_2O. The chemical structures of the adsorbent, metal ion in solution, adsorbent-metal complex,

and H_2O were drawn with AVOGADRO and pre-optimized. However, for an easy simulation, the ionic interaction of protonated chitosan with ions of pyridine-2,6-dicarboxylate was replaced with a peptide linkage as the interaction can as well occur through condensation by the elimination of water molecule. The charges on the metal ions were taken into consideration, and where necessary, the spin multiplicities were assigned base on a strong field ligand for the adsorbent-metal and a weak field ligand for the metal ions in solution. Thereafter, geometry optimization of the chemical structures was performed using ORCA at the RI-PB/def2-SVP level of theory with the aim of obtaining the final single point energies. The adsorption energy (E_{ads}) was calculated as follows:

$$E_{ads} = [E(\text{adsorbent-metal}_{(s)}) + E(nH_2O)] - [E(\text{adsorbent}_{(s)}) + E(\text{metal}_{(aq)})] \quad (8)$$

Where $E(\text{adsorbent-metal}_{(s)})$ is the final single point energy (FSE) of the adsorbent bound metal, $E(nH_2O)$ is the FSE of n molecules of water, $E(\text{adsorbent}_{(s)})$ is the FSE of the adsorbent (PDC-CCS) and $E(\text{metal}_{(aq)})$ is the FSE of metal ion in solution.

Table 1: Result of FSE for the adsorbent, metal ions in solution [$\text{metal}_{(aq)}$], adsorbent bound-metal [$\text{adsorbent-metal}_{(s)}$], 6$H_2O$ and adsorption energy.

$E_{adsorbent(s)}$ (Eh)	$E_{metal(aq)}$ (Eh)	$E_{adsorbent-metal(s)}$ (Eh)	$6(EH_2O)$ (Eh)	Adsorption energy (Eh)
	Cu(II)			
-3459.0801	-2098.2197	-5099.1858	-458.1648	-0.0508
	Ni(II)			
-3459.0801	-1966.1280	-4967.0907	-458.1648	-0.0474
	Cd(II)			
-3459.0801	-625.5834	-3626.5422	-458.1648	-0.0435
	Pb(II)			
-3459.0801	-650.3730	-3651.2985	-458.1648	-0.0103
	Mn(II)			
-3459.0801	-1608.8333	-4609.751	-458.1648	-0.0024

	Cr(III)			
-3459.0801	-1501.6064	-4502.5*	-458.1648	0.0217

*: Optimization energy not converged after 3000 iterations

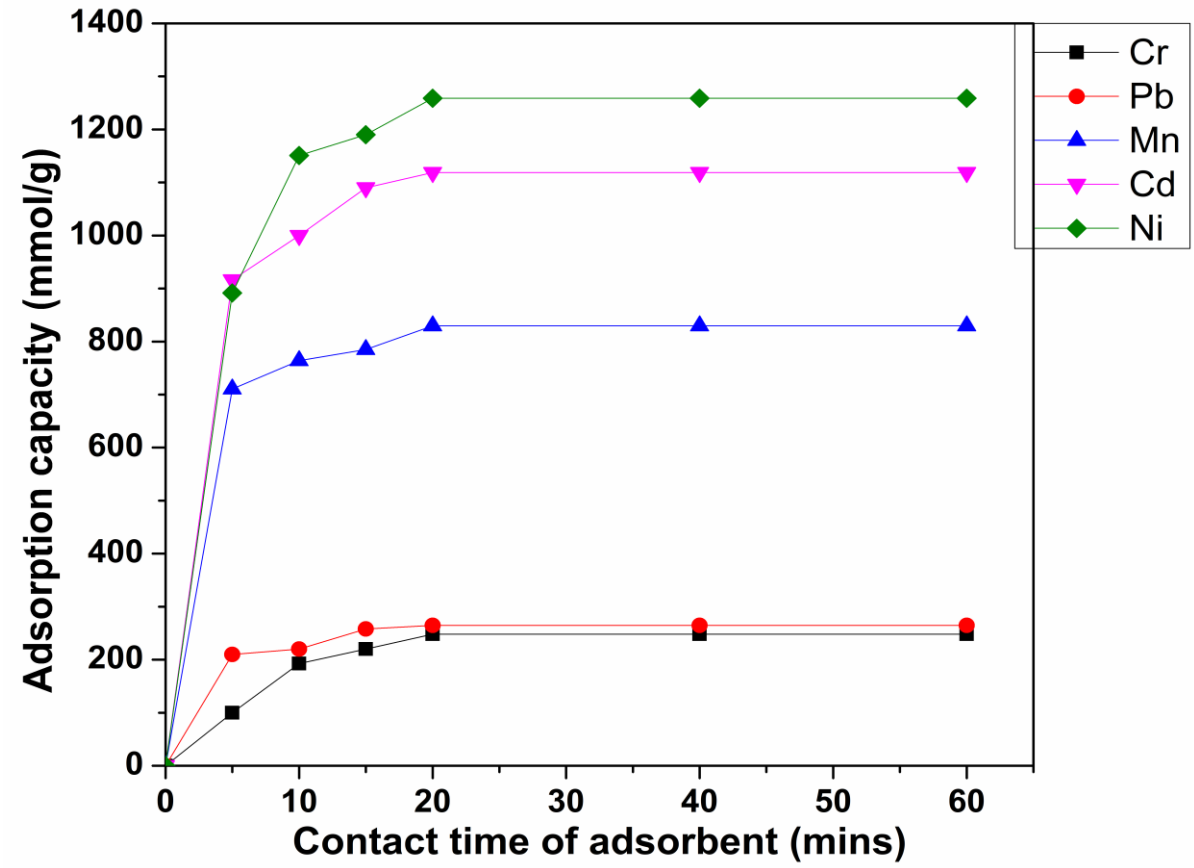

Figure 2: Capacity of adsorption of PDC-CCS for Cr^{3+}, Pb^{2+}, Mn^{2+}, Cd^{2+}, and Ni^{2+} [at 30 °C, pH 7.5, initial metal ion concentration of 2.5 mmol/l]

The adsorption process is illustrated in scheme 1 where the metal ions are chelated by the O and N donor sites on the adsorbent mainly by the transfer of charge from the adsorbent to the metal ions in solution, as indicated by the NPA charge obtained from the Natural bond orbital (NBO) calculations [45]. Figure 2 shows the result obtained when PDC-CCS was used to remove other toxic metals [Cd(II), Cr(III), Mn(II), Pb(II), and Ni(II)] from water at the observed optimum adsorption conditions for Cu(II). The decrease in adsorbent's capacity of adsorption for the metals as illustrated in figure 2 is as follows: $Ni^{2+} > Cd^{2+} > Mn^{2+} > Pb^{2+} > Cr^{3+}$. However, the result of the computational studies suggested that the PDC-CCS's capacity of adsorption for Pb(II) would be higher than the result obtained in figure 2 since the adsorption energy for Pb(II) is less than Mn(II), as illustrated in table 1. This has necessitated the study of the adsorption behaviour of PDC-CCS towards the metal ions [Pb(II), Cr(III), Mn(II), Cd(II),

and Ni(II)] at varying pH (i.e., pH 7.5, 6.65, 5.56, and 4.20). While the adsorption capacity of PDC-CCS for Mn(II), Cd(II), and Ni(II) increases with an increase in pH, the adsorption capacity of PDC-CCS for Pb(II) and Cr(III) increases with a decrease in pH (as shown in the supplementary information figures S1, S2, and S3). Thus, the optimum adsorption capacity of PDC-CCS for the metals is in the order: $Ni^{2+} > Cd^{2+} > Pb^{2+} > Mn^{2+} > Cr^{3+}$ and with experimental values of 1258.79, 1118.70, 928.52, 829.62, and 580.21 mmol/g respectively.

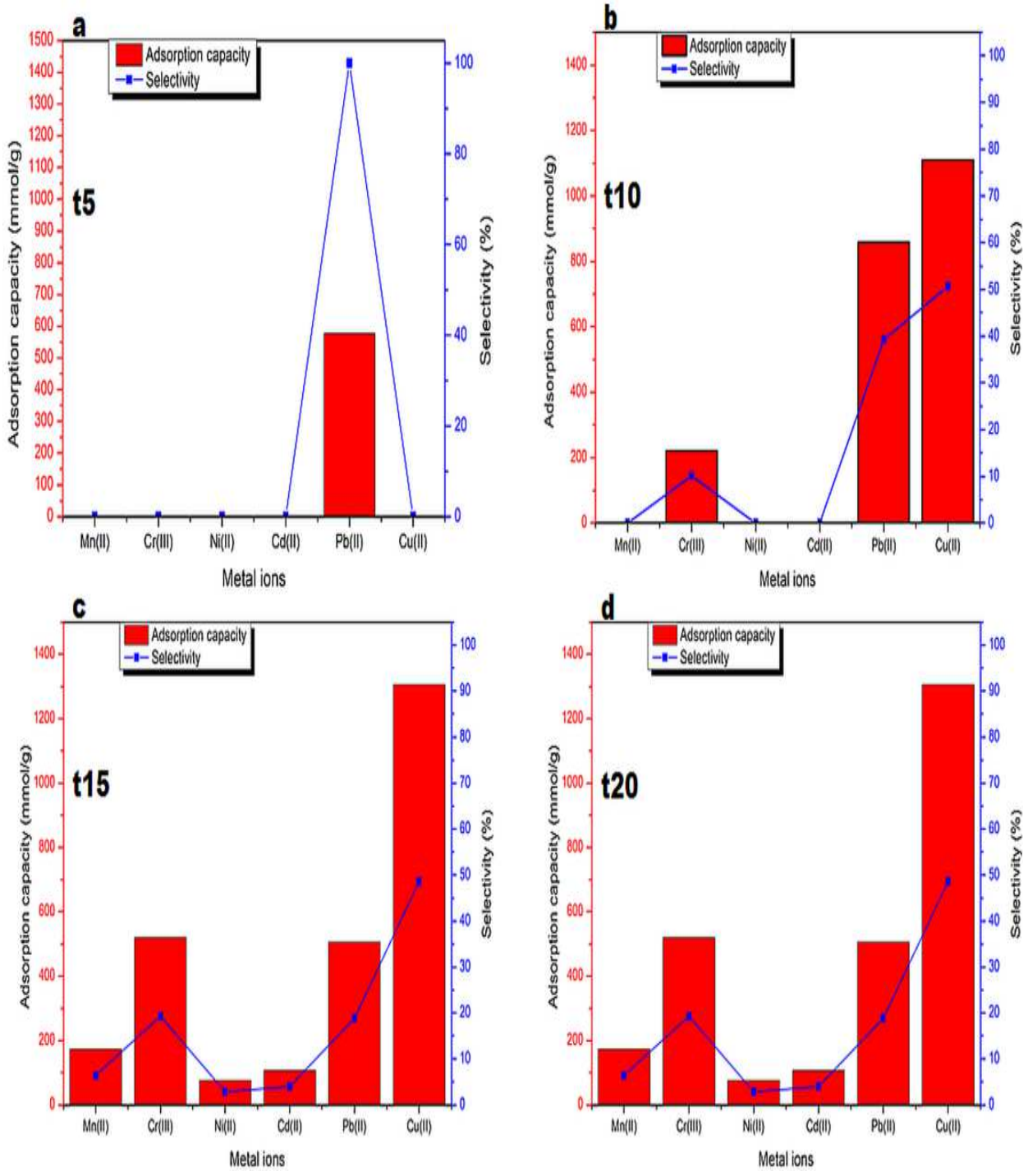

Figure 3: Competitive adsorption capacities and selectivity of PDC-CCS at pH 4.2 for Mn^{2+}, Cr^{3+}, Ni^{2+}, Cd^{2+}, Pb^{2+}, and Cu^{2+} within; (a) five mins (b) ten mins (c) fifteen mins and (d) twenty mins.

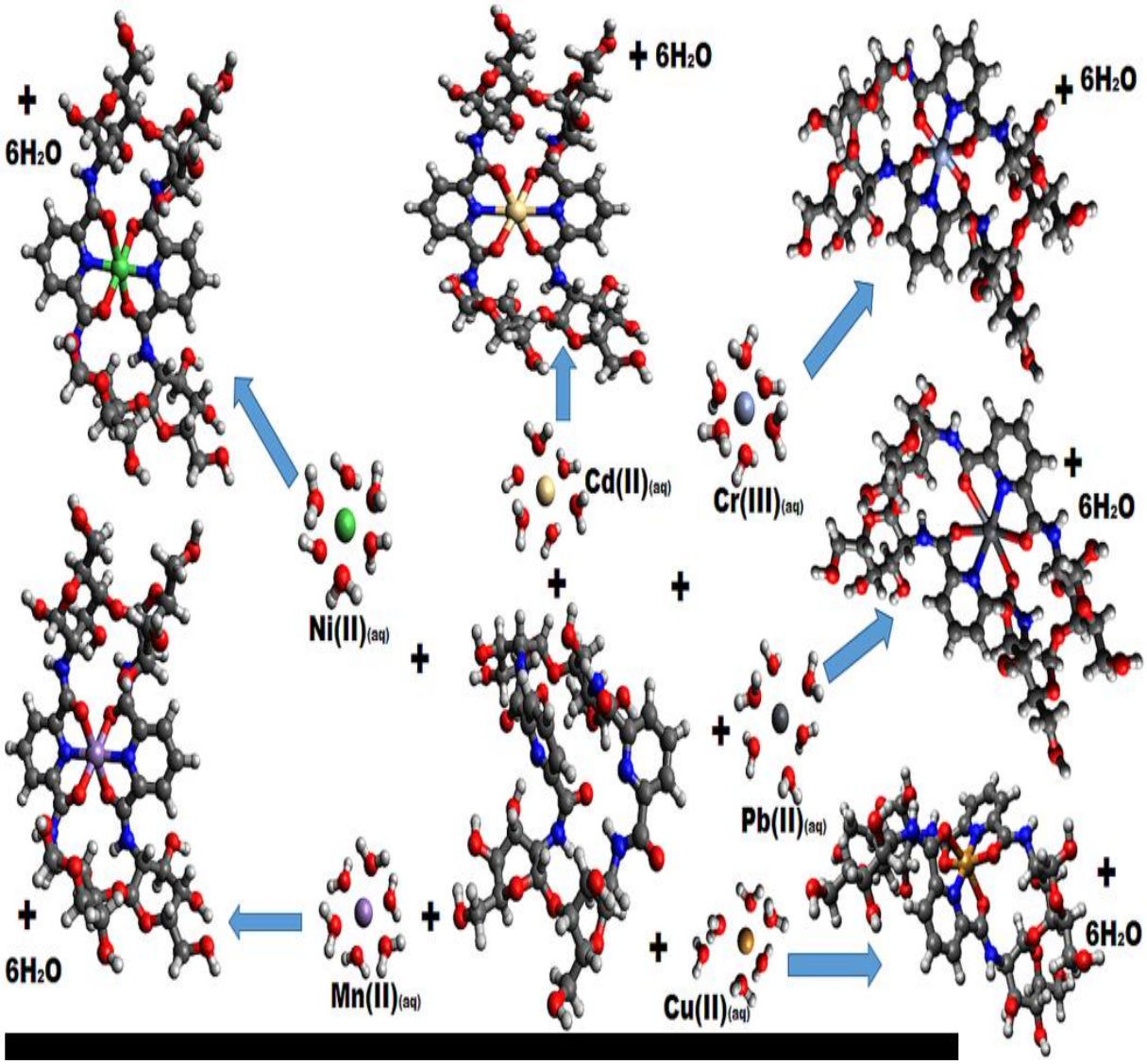

Scheme 1: Adsorption process of the metal ions [Mn^{2+}, Cr^{3+}, Ni^{2+}, Cd^{2+}, Pb^{2+} and Cu^{2+}] on the adsorbent [PDC-CCS] via chelation/complexation

The Langmuir and the Freundlich adsorption isotherms are shown in figures S4 and S5 (Supplementary information), respectively, while the *pseudo*-first-order and second-order kinetic models are shown in figure S6 and S7, respectively. Although the experimental adsorption process suits the Langmuir and Freundlich adsorption isotherms based on the R^2 values (Table S1 supplementary information), the adsorption process can best be described using the Langmuir approach if the Q_m and K_F (in table S1) are compared with the experimental maximum adsorption capacity. Also, based on the R^2 values (in table S2), the second-order kinetic model closely suits the adsorption of Cu(II) and the other toxic metals on the adsorbent (PDC-CCS), thus suggesting chemisorption in which the metal ions are mainly adsorbed through complexation by the various donor sites on the adsorbent[45]

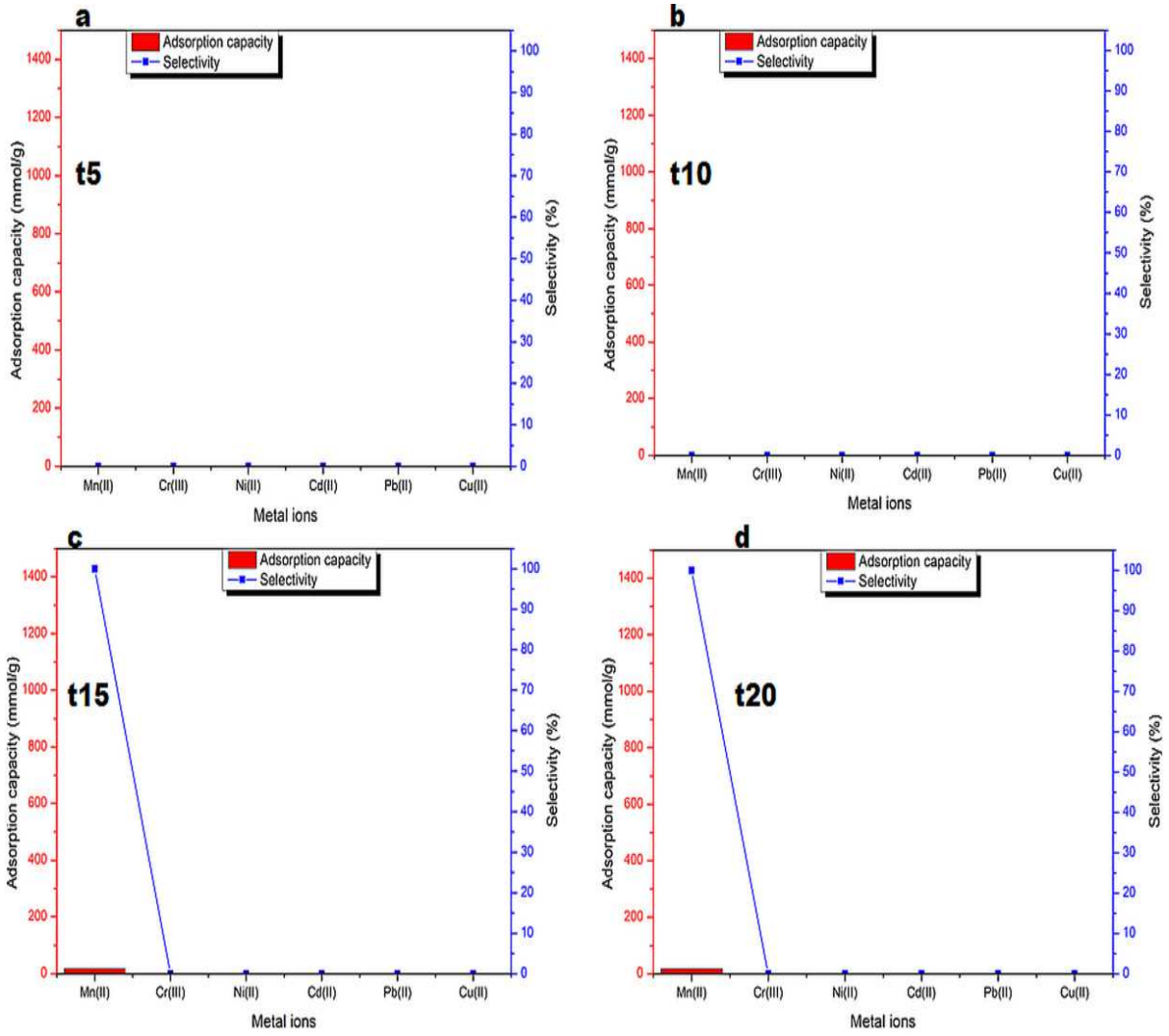

Figure 4: Competitive adsorption capacities and selectivity of PDC-CCS at pH 5.6 for Mn^{2+}, Cr^{3+}, Ni^{2+}, Cd^{2+}, Pb^{2+}, and Cu^{2+} within; (a) five mins (b) ten mins (c) fifteen mins and (d) twenty mins.

Additionally, the competitive adsorption capacities and selectivity of PDC-CCS for the metals at pH 4.20, 5.56, 6.65, and 7.61 are shown in figures 3, 4, 5, and 6, respectively. The selectivity studies show that the adsorbent (PDC-CCS) has the tendency to adsorb all the competing metal ions within 15 minutes of contact time at a pH of 4.2 (figure 3). The capacity of adsorption and adsorbent's selectivity towards the metal ions are in the following order: $Cu^{2+} > Pb^{2+} > Cr^{3+} > Mn^{2+} > Cd^{2+} > Ni^{2+}$. However, at pH 5.56 (figure 4), the tendency of the adsorbent to adsorb the metal ions in solution decreases but with high selectivity (100%) towards Mn(II). The observed reduction in adsorption capacity at the pH of 5.56 may be due to the strong competition among the metal ions for uptake by the adsorbent. In essence, as one metal ion is adsorbed, it is replaced by another metal ion; the process continues until an equilibrium is

attained when a small amount of Mn(II) is successfully adsorbed without replacement after 15 minutes of contact time.

In the same vein, the regeneration and reusability of the adsorbent (PDC-CCS) have been examined on the adsorption of the toxic metal ions following the previous method [45]. The result obtained is illustrated in figure S8 (Supplementary Information). From this result, it is clear that the adsorbent can be used for several cycles of adsorption studies.

Table 2: Comparison between PDC-CCS adsorption capability and some previously recorded relevant adsorbents

Author/year	Adsorbent	Adsorption Capacity	Reference
	Ni(II)		
Cuiping Wang et al. (2012)	Tourmaline	13.10 mg/g	[50]
Guanhao Liu et al. (2009)	Mg-Al Hydrotalcites Intercalated by ethylenediaminetetraacetic acid	108.20 mg/g	[51]
Debashis kundu et al. (2019)	β-Cyclodextrin-Cellulose/Hemi cellulose-Based Hydrogels	15.93 mg/g	[52]
Liping Fang et al. (2015)	LDH – HA	480.40 mg/g	[53]
	LDH – FA	290.60 mg/g	
Sayed Zia Mohammadi et al. (2014)	Activated Carbon from *Glycyrrhiza glabra* residue	166.70 mg/g	[54]
Eveliina Repo et al. (2009)	Silica gel functionalized with EDTA	21.60 mg/g	[55]
	DTPA-modified silica gel	16.70 mg/g	
Vinod Kumar Gupta et al. (2014)	Scrap tyre	25 mg/g	[56]
Wei Shen et al. (2019)	Alginate modified graphitic carbon nitride hydrogels	306.30 mg/g	[57]
Dawodu and Akpomie (2014)	Nigerian Kaolinite clay	166.67 mg/g	[58]

Ibraheem and Reinout (2020)	PDC-CCS	1258.79 mmol/g	This work
	Cd(II)		
Cuiping Wang et al. (2012)	Tourmaline	25.19 mg/g	[50]
Debashis kundu et al. (2019)	β-Cyclodextrin-Cellulose/Hemi cellulose-Based Hydrogels	24.66 mg/g	[52]
Jayabrata and Samit	Biocomposite Hydrogel	193.90 mg/g	[59]
Rashi Gusain et al. (2019)	(M_oS)/thiol functionalized multiwalled carbon nanotube (SH-MWCNT)	66.60 mg/g	[60]
Diana Cholico-Gonzalez et al. (2020)	Agave Bagasse	28.50 mg/g	[61]
Xiong Yang et al. (2020)	Birnessite	239.7 mg/g	[62]
Pu Yang et al. (2020)	Ion-imprinted polymers	41.212 mg/g	[63]
Fudong Wang et al. (2019)	Straw Cellulose Hydrogel Beads ($SCHB_s$)	95.62 mg/g	[64]
Jianhua Guo et al. (2019)	HA/Fe-Mn Oxides-loaded biochar composite (HFMB)	67.11 mg/g	[65]
Emmanuel F. Olasehinde et al. (2019)	Onion skin	21.28 mg/g	[66]
Ibraheem and Reinout (2020)	PDC-CCS	1118.70 mmol/g	This work
	Pb(II)		
Rashi Gusain et al. (2019)	(M_oS)/thiol functionalized multiwalled carbon nanotube (SH-MWCNT)	90.00 mg/g	[60]
Sukanya Kundu et al (2018)	Nitrogen-Doped Nanoporous Carbon Nanospheroids	99.82 mg/g	[67]
Said Tighadouini et al (2019)	Pyridylpyrazole-β-ketenol Receptor Covalently Bonded onto the Silica Surface	110.84 mg/g	[68]

Diana Cholico-Gonzalez et al (2020)	Agave Bagasse	93.14 mg/g	[61]
Wei Shen et al. (2019)	Alginate modified graphitic carbon nitride hydrogels	383.40 mg/g	[57]
Sayed Zia Mohammadi et al. (2014)	Activated Carbon from *Glycyrrhiza glabra* residue	200.00 mg/g	[54]
Ibraheem and Reinout (2020)	PDC-CCS	928.52 mmol/g	This work
	Mn(II)		
Han Yan et al. (2014)	Magnetic grapheme oxide	16.5 mg/g	[69]
Dawodu and Akpomie (2014)	Nigerian Kaolinite clay	111.11 mg/g	[58]
Z. Abdeen et al. (2015)	Polyvinyl alcohol/Chitosan (PVA/CS)	10.515 mg/g	[70]
Yong Liu et al. (2017)	Magnetic Fe_3O_4 nano-particles	36.81 mg/g	[71]
Xiangbing Zhu et al. (2016)	Diethylenetriamine-functionalized carbon nanotubes dispersed in grapheme oxide colloids	9.5 mg/g	[72]
Mingjie Huang et al. (2019)	Layered doubled hydroxide intercalated with diethylene triamine pentaacetic acid (LDH_s-DTPA)	83.5 mg/g	[73]
	LDH_s-EDTA	44.4 mg/g	
	LDH_s-Oxalate	21.6 mg/g	
	LDH_s	28.8 mg/g	
Zhangxiang Lin et al. (2020)	Zeolite	8.6 mg/g	[74]
Ramin Mohammadi et al. (2019)	Alginate-Combusted coal gangue composite	64.29 mg/g	[75]
Seung-Moklee et al. (2009)	Manganese-coated sand sample (MCS)	59.34 mg/g	[76]

Ibraheem and Reinout (2021)	PDC-CCS	829.62 mmol/g	This work
	Cr(III)		
Mohammad et al (2005)	Ultrasound and Discarded Tire Rubber	1.11 mg/g	[77]
Arnab Dutta et al (2020)	AMPS-co-APMPS-co-AM AA-co-APA-co-AM MAA-co-AMPA-co-AM	1316.35 mg/g 1431.40 mg/g 1372.18 mg/g	[78]
Ibraheem and Reinout (2020)	PDC-CCS	580.21 mmol/g	This work

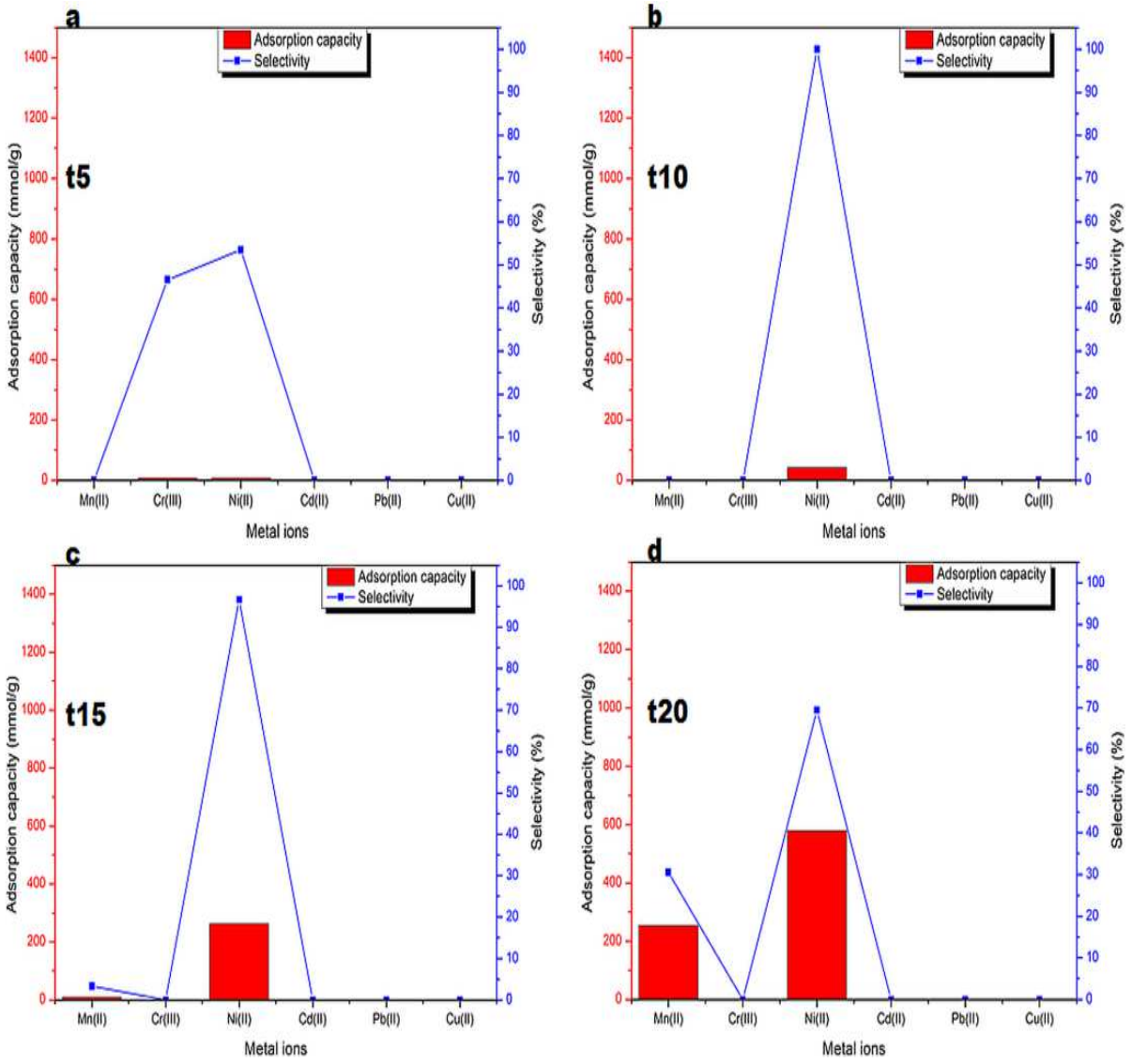

Figure 5: Competitive adsorption capacities and selectivity of PDC-CCS at pH 6.65 for Mn^{2+}, Cr^{3+}, Ni^{2+}, Cd^{2+}, Pb^{2+}, and Cu^{2+} within; (a) five mins (b) ten mins (c) fifteen mins and (d) twenty mins.

Similarly, the selectivity of PDC-CCS shifted towards Ni(II) and Mn(II) near-neutral pH (i.e., pH 6.65 and 7.61 as seen in figures 5 and 6, respectively. A small amount of Cr(III) was initially adsorbed but was replaced within 15 minutes of contact time. However, PDC-CCS adsorbed more Ni(II) than Mn(II) at both pH values.

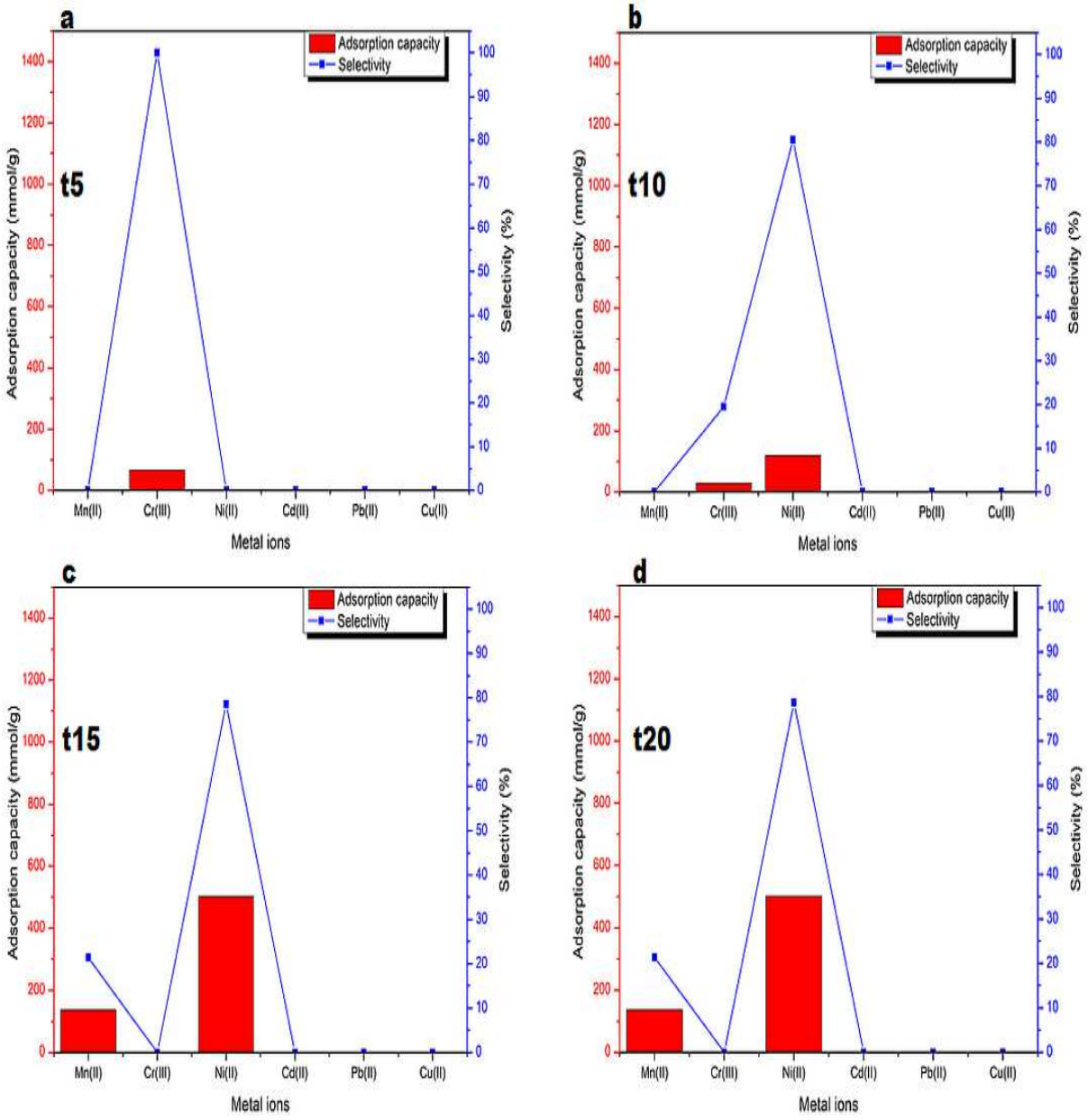

Figure 6: Competitive adsorption capacities and selectivity of PDC-CCS at pH 7.61 for Mn^{2+}, Cr^{3+}, Ni^{2+}, Cd^{2+}, Pb^{2+}, and Cu^{2+} within; (a) five mins (b) ten mins (c) fifteen mins and (d) twenty mins.

Interestingly, PDC-CCS shows exceptional adsorption capacity towards metal ions compared to some of the applicable adsorbents previously published, as shown in table 2.

Conclusion

The adsorption of Cd^{2+}, Cr^{3+}, Mn^{2+}, $Pb^{2+,}$ and Ni^{2+} utilizing 2,6-pyridinedicarboxylic acid crosslinked chitosan (PDC-CCS) has been discussed. The capacity of adsorption by PDC-CCS was investigated at pH 7.5, while adsorption selectivities were examined at pH 4.2, 5.56, 6.65, and 7.61. The density functional theory approach has been used to support the trend in adsorption capacities of PDC-CCS for the metal ions. Results obtained indicate that PDC-CCS is a novel biopolymer adsorbent which can be employed for the simultaneous removal of toxic metals and selective removal of Mn(II) from water.

Conflicts of interest

There are no disputes to report.

Acknowledgement

The financial support provided for this research from The World Academy of Sciences (TWAS) in partnership with the National Research Foundation (NRF) is hereby recognized. The views expressed and the conclusions drawn are those of the author and are not inherently attributable to the NRF-TWAS.

References

[1] K. R. Krishnapriya and M. Kandaswamy, Carbohydrate Research 345 (2010) 2013.

[2] C. A. Rodrigues, M. C. M. Laranjeira, V. T. de Fávere and E. Stadler, Polymer 39 (1998) 5121.

[3] W. S. Wan Ngah, L. C. Teong and M. A. K. M. Hanafiah, Carbohydrate Polymers 83 (2011) 1446.

[4] A. K. Bajpai, Journal of Water Process Engineering 32 (2019) 100920.

[5] P. Baroni, R. S. Vieira, E. Meneghetti, da Silva, M. G. C. and M. M. Beppu, J. Hazard. Mater. 152 (2008) 1155.

[6] A. Chen, S. Liu, C. Chen and C. Chen, J. Hazard. Mater. 154 (2008) 184.

[7] M. L. P. Dalida, A. F. V. Mariano, C. M. Futalan, C. Kan, W. Tsai and M. Wan, Desalination 275 (2011) 154.

[8] S. Dandil, D. Akin Sahbaz and C. Acikgoz, Int. J. Biol. Macromol. 136 (2019) 668.

[9] S. Ding, X. Zhang, X. Feng, Y. Wang, S. Ma, Q. Peng and W. Zhang, React Funct Polym 66 (2006) 357.

[10] H. Ge, T. Hua and X. Chen, J. Hazard. Mater. 308 (2016) 225.

[11] H. Ge and T. Hua, Carbohydr. Polym. 153 (2016) 246.

[12] P. Gogoi, A. J. Thakur, R. R. Devi, B. Das and T. K. Maji, Journal of Environmental Chemical Engineering 4 (2016) 4248.

[13] B. Hastuti and Y. Santrinitas, Materials Science Forum 890 (2017) 171.

[14] C. Jiang, X. Wang, G. Wang, C. Hao, X. Li and T. Li, Composites Part B: Engineering 169 (2019) 45.

[15] T. Kameda, R. Honda, S. Kumagai, Y. Saito and T. Yoshioka, Journal of Solid State Chemistry 277 (2019) 143.

[16] M. Kumar, B. P. Tripathi and V. K. Shahi, J. Hazard. Mater. 172 (2009) 1041.

[17] R. Laus, T. G. Costa, B. Szpoganicz and V. T. Fávere, J. Hazard. Mater. 183 (2010) 233.

[18] Y. Li, M. Li, J. Zhang and X. Xu, Chinese Chemical Letters 30 (2019) 762.

[19] Manasi, V. Rajesh and N. Rajesh, Int. J. Biol. Macromol. 79 (2015) 300.

[20] S. Mallakpour and E. Khadem, Sci. Total Environ. 690 (2019) 1245.

[21] J. S. Marques, M. R. Pereira, A. Sotto and J. M. Arsuaga, Reactive and Functional Polymers 134 (2019) 31.

[22] J. Mei, H. Zhang, Z. Li and H. Ou, Carbohydr. Polym. 224 (2019) 115154.

[23] L. Midya, R. Das, M. Bhaumik, T. Sarkar, A. Maity and S. Pal, J. Colloid Interface Sci. 542 (2019) 187.

[24] W. S. W. Ngah and S. Fatinathan, Journal of Environmental Sciences 22 (2010) 338.

[25] M. L. Nguyen and R. Juang, Journal of the Taiwan Institute of Chemical Engineers 56 (2015) 96.

[26] P. A. Nishad, A. Bhaskarapillai and S. Velmurugan, Carbohydr. Polym. 108 (2014) 169.

[27] A. A. Radwan, F. K. Alanazi and I. A. Alsarra, Molecules (Basel, Switzerland) 15 (2010) 6257.

[28] Rahmi, Lelifajri and R. Nurfatimah, Carbohydr. Polym. 199 (2018) 499.

[29] A. Ramesh, H. Hasegawa, W. Sugimoto, T. Maki and K. Ueda, Bioresource Technology 99 (2008) 3801.

[30] S. P. Ramnani and S. Sabharwal, Reactive and Functional Polymers 66 (2006) 902.

[31] G. Sharma, M. Naushad, A. H. Al-Muhtaseb, A. Kumar, M. R. Khan, S. Kalia, Shweta, M. Bala and A. Sharma, Int. J. Biol. Macromol. 95 (2017) 484.

[32] A. Shekhawat, S. Kahu, D. Saravanan and R. Jugade, Int. J. Biol. Macromol. 80 (2015) 615.

[33] T. Shi, D. Yang, H. Yang, J. Ye and Q. Cheng, Appl. Clay. Sci. 142 (2017) 100.

[34] S. Sun, L. Wang and A. Wang, J. Hazard. Mater. 136 (2006) 930.

[35] Z. A. Sutirman, M. M. Sanagi, K. J. Abd Karim and W. A. Wan Ibrahim, Carbohydr. Polym. 151 (2016) 1091.

[36] Z. A. Sutirman, M. M. Sanagi, J. Abd Karim, A. Abu Naim and W. A. Wan Ibrahim, Int. J. Biol. Macromol. 107 (2018) 891.

[37] V. N. Tirtom, A. Dinçer, S. Becerik, T. Aydemir and A. Çelik, Chem. Eng. J. 197 (2012) 379.

[38] M. Vakili, S. Deng, T. Li, W. Wang, W. Wang and G. Yu, Chem. Eng. J. 347 (2018) 782.

[39] H. L. Vasconcelos, T. P. Camargo, N. S. Gonçalves, A. Neves, M. C. M. Laranjeira and V. T. Fávere, React Funct Polym 68 (2008) 572.

[40] F. C. Vicentini, T. A. Silva, A. Pellatieri, B. C. Janegitz, O. Fatibello-Filho and R. C. Faria, Microchemical Journal 116 (2014) 191.

[41] R. S. Vieira and M. M. Beppu, Colloids Surf. Physicochem. Eng. Aspects 279 (2006) 196.

[42] R. S. Vieira, M. L. M. Oliveira, E. Guibal, E. Rodríguez-Castellón and M. M. Beppu, Colloids Surf. Physicochem. Eng. Aspects 374 (2011) 108.

[43] Y. Yan, G. Yuvaraja, C. Liu, L. Kong, K. Guo, G. M. Reddy and G. V. Zyryanov, International Journal of Biological Macromolecules 117 (2018) 1305.

[44] N. Zhang, H. Zhang, R. Li and Y. Xing, International journal of biological macromolecules 152 (2020) 1146.

[45] I. O. Bisiriyu and R. Meijboom, Int. J. Biol. Macromol. 165 (2020) 2484.

[46] D. T. Thien, N. T. An and N. T. Hoa, Chemical Sciences Journal 6 (2015) 95.

[47] Renata Czechowska-Biskup, Diana Jarosińska, Bożena Rokita, Piotr Ulański and Janusz M. Rosiak, Progress on Chemistry 12 (2012) 5.

[48] T. Wu and S. Zivanovic, Carbohydrate Polymers 73 (2008) 248.

[49] G. Sailakshmi, T. Mitra, S. Chatterjee and A. Gnanamani, Journal of Biomaterials and Nanobiotechnology 4 (2013) 151.

[50] C. Wang, J. Liu, Z. Zhang, B. Wang and H. Sun, Industrial & Engineering Chemistry Research 51 (2012) 4397.

[51] G. Liu, J. Yang, X. Xu and Z. He, Journal of Chemical & Engineering Data 64 (2019) 5838.

[52] D. Kundu, S. K. Mondal and T. Banerjee, Journal of Chemical & Engineering Data 64 (2019) 2601.

[53] L. Fang, W. Li, H. Chen, F. Xiao, L. Huang, P. E. Holm, H. C. B. Hansen and D. Wang, RSC Advances 5 (2015) 18866.

[54] S. Z. Mohammadi, H. Hamidian and Z. Moeinadini, Journal of Industrial and Engineering Chemistry 20 (2014) 4112.

[55] E. Repo, T. A. Kurniawan, J. K. Warchol and M. E. T. Sillanpää, Journal of Hazardous Materials 171 (2009) 1071.

[56] V. K. Gupta, Suhas, A. Nayak, S. Agarwal, M. Chaudhary and I. Tyagi, Journal of Molecular Liquids 190 (2014) 215.

[57] W. Shen, Q. An, Z. Xiao, S. Zhai, J. Hao and Y. Tong, International journal of biological macromolecules 148 (2020) 1298.

[58] F. A. Dawodu and K. G. Akpomie, Journal of Materials Research and Technology 3 (2014) 129.

[59] J. Maity and S. K. Ray, The Journal of Physical Chemistry B 121 (2017) 10988.

[60] R. Gusain, N. Kumar, E. Fosso-Kankeu and S. S. Ray, ACS Omega 4 (2019) 13922.

[61] D. Cholico-González, N. Ortiz Lara, A. M. Fernández Macedo and J. Chavez Salas, ACS omega 5 (2020) 3302.

[62] X. Yang, Q. Peng, L. Liu, W. Tan, G. Qiu, C. Liu and Z. Dang, Chemosphere 247 (2020) 125822.

[63] P. Yang, H. Cao, D. Mai, T. Ye, X. Wu, M. Yuan, J. Yu and F. Xu, Reactive and Functional Polymers 151 (2020) 104569.

[64] F. Wang, J. Li, Y. Su, Q. Li, B. Gao, Q. Yue and W. Zhou, Journal of Industrial and Engineering Chemistry 80 (2019) 361.

[65] J. Guo, C. Yan, Z. Luo, H. Fang, S. Hu and Y. Cao, Journal of Environmental Sciences 85 (2019) 168.

[66] E. F. Olasehinde, A. V. Adegunloye, M. A. Adebayo and A. A. Oshodi, Water Conservation Science and Engineering 4 (2019) 175.

[67] S. Kundu, I. H. Chowdhury and M. K. Naskar, ACS Omega 3 (2018) 9888.

[68] S. Tighadouini, S. Radi, M. Ferbinteanu and Y. Garcia, ACS omega 4 (2019) 3954.

[69] H. Yan, H. Li, X. Tao, K. Li, H. Yang, A. Li, S. Xiao and R. Cheng, ACS Applied Materials & Interfaces 6 (2014) 9871.

[70] Z. Abdeen, S. G. Mohammad and M. S. Mahmoud, Environmental Nanotechnology, Monitoring & Management 3 (2015) 1.

[71] Y. Liu, J. Bai, H. Duan and X. Yin, Chinese Journal of Chemical Engineering 25 (2017) 32.

[72] X. Zhu, Y. Cui, X. Chang and H. Wang, Talanta 146 (2016) 358.

[73] M. Huang, Y. Zhang, W. Xiang, T. Zhou, X. Wu and J. Mao, Journal of Environmental Sciences 90 (2020) 411.

[74] Z. Lin, P. Yuan, Y. Yue, Z. Bai, H. Zhu, T. Wang and X. Bao, Science of the Total Environment 698 (2020) 134287.

[75] R. Mohammadi, A. Azadmehr and A. Maghsoudi, Journal of Environmental Chemical Engineering 7 (2019) 103494.

[76] S. Lee, D. Tiwari, K. Choi, J. Yang, Y. Chang and H. Lee, Journal of Chemical & Engineering Data 54 (2009) 1823.

[77] M. H. Entezari, N. Ghows and M. Chamsaz, The Journal of Physical Chemistry A 109 (2005) 4638.

[78] A. Dutta, M. Mahapatra, M. Deb, M. Mitra, S. Dutta, P. K. Chattopadhyay, S. Banerjee, P. C. Sil, D. K. Maiti and N. R. Singha, ACS biomaterials science & engineering 6 (2020) 1397.

Supplementary Files

This is a list of supplementary files associated with this preprint. Click to download.

- SupplementaryinformationM3.docx